

$^{233}\text{U}(n,F)$ Prompt Fission Neutron Spectra

V.M. Maslov*

220025 Minsk, Byelorussia

*E-mail: mvm2386@yandex.ru

Simultaneous analysis of measured data for $^{235}\text{U}(n,F)$, $^{239}\text{Pu}(n,F)$ and $^{233}\text{U}(n,F)$ maintains stronger justification for the predicted prompt fission neutron spectra (PFNS) of $^{233}\text{U}(n,F)$. Pre-fission neutrons influence the partitioning of fission energy between excitation energy and total kinetic energy of fission fragments. For the reactions $^{233}\text{U}(n,F)$ and $^{235}\text{U}(n,F)$ shape of prompt fission neutron spectra strongly depends on relative positions of (n,xnf) and (n,xn) reaction thresholds. The correlation of these peculiarities with emissive fission contributions (n,xnf) to the $\sigma_{n,F}$ and competition of reactions $(n,n\gamma)$ and $(n,xn)^{1\dots x}$ is established. Exclusive neutron spectra $(n,xnf)^{1\dots x}$ are consistent with $\sigma_{n,F}$ of $^{233}\text{U}(n,F)$ and $^{232}\text{U}(n,F)$. Initial model parameters for $^{233}\text{U}(n,F)$ PFNS are fixed by description of PFNS of $^{233}\text{U}(n_{th},F)$ and ratios of PFNS of $^{233}\text{U}(n_{th},F)/^{235}\text{U}(n_{th},F)$ and $^{239}\text{Pu}(n_{th},F)/^{233}\text{U}(n_{th},F)$. We predict the $^{233}\text{U}(n,xnf)^{1\dots x}$ exclusive pre-fission neutron spectra, exclusive neutron spectra of $^{233}\text{U}(n,xn)^{1\dots x}$ reactions, total kinetic energy TKE of fission fragments and products, observed and partials of average prompt fission neutron number and observed PFNS of $^{233}\text{U}(n,F)$.

INTRODUCTION

Fissile nuclides ^{233}U may build-up in breeder or hybrid reactors. Nuclear data for $^{233}\text{U}+n$ interaction, with the exception for $\sigma_{n,F}$ data, are scarce, especially as regards PFNS $S(\varepsilon, E_n)$ of $^{233}\text{U}(n,F)$ in the range of $^{233}\text{U}(n,xnf)^{1\dots x}$ reaction. Data on PFNS $S(\varepsilon, E_n)$ at $E_n \sim 14.3$ MeV [1] remained the only available before long. Since model analysis in [1] was then over-simplified, relative contributions of pre- and post-fission neutrons in [1] disagree with later predictions [2, 3]. Measured data at $E_n \sim E_{th}$ [4], $E_n \sim 0.55$ MeV [5], and data [1] as well, were abandoned in all versions of BROND/ROSFOND, ENDF/B, JEFF and JENDL data libraries. The data of recent PFNS measurements for $^{233}\text{U}(n_{th},f)$ [6], $^{235}\text{U}(n_{th},f)$ and $^{239}\text{Pu}(n_{th},f)$ [6, 7] are discrepant with the data of [4]. Lumping [4, 6, 7] data in a spline fitting procedure of [8] would change predicted PFNS shapes of $^{233}\text{U}(n_{th},f)$, $^{235}\text{U}(n_{th},f)$ and $^{239}\text{Pu}(n_{th},f)$ drastically (see Fig. 1).

In differential PFNS data for ^{235}U and ^{239}Pu for $E_n \sim 1.5\text{--}20$ MeV and $\varepsilon \sim 0.01\text{--}10$ MeV [9–11] strong variations of average PFNS energies $\langle E \rangle$ were observed around (n,xnf) thresholds. $\langle E \rangle$ is rough signature of PFNS, however it was established in [9–11] that the relative amplitude of $\langle E \rangle$ variation in case of $^{239}\text{Pu}(n,F)$ reaction is much weaker than in case of $^{235}\text{U}(n,F)$. That is due to influence of (n,xnf) reactions on fission observables when fission is preceded by pre-fission neutrons. In case of $^{233}\text{U}(n,F)$ reactions similar variations of $\langle E \rangle$ were predicted in [2, 3, 8]. We intend to predict PFNS of $^{233}\text{U}(n,F)$ at $E_n \sim E_{th}\text{--}20$ MeV.

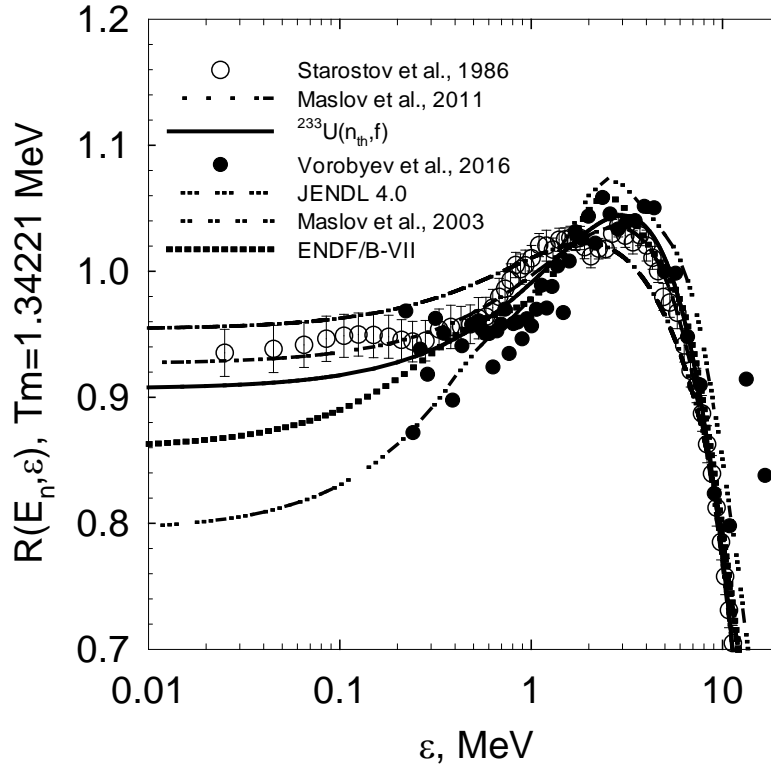


Fig.1. Prompt fission neutron spectra of $^{233}\text{U}(n_{th},f)$ relative to Maxwellian, $\langle E \rangle = 2.0564$ MeV.

$^{233}\text{U}(n,f)$ PROMPT FISSION NEUTRONS

Recent PFNS data for $^{233}\text{U}(n_{th},f)$ [6] added even more controversy: at range $0.02 < \varepsilon < 5$ MeV they support the evaluations of ENDF/B-VII [12] and JENDL-4.0 [13], while PFNS of both libraries disagree with data [4]. Data [4] are presented as spline approximation of [8], which summons empirical features of consistent analysis of $^{233}\text{U}(n_{th},f)$, $^{235}\text{U}(n_{th},f)$, $^{239}\text{Pu}(n_{th},f)$ and $^{252}\text{Cf}(sf)$ measured PFNS data [4]. In the energy range $5 < \varepsilon < 11$ MeV data of [6] for $^{233}\text{U}(n,f)$ support the evaluation of [8], which is based on data [4] fitting at $0.02 < \varepsilon < 9.3$ MeV.

The comparison of PFNS measured data [4, 6, 7, 9–11] for $^{233}\text{U}(n,f)$, $^{235}\text{U}(n,f)$ and $^{239}\text{Pu}(n,f)$ in the range $E_{th} < E_n < E_{mf}$ shows that enhanced soft neutron yield, $\varepsilon \lesssim 1$ MeV is a common feature except PFNS of [6, 7]. In [6, 7] PFNS of $^{233}\text{U}(n_{th},f)$, $^{235}\text{U}(n,f)$ and $^{239}\text{Pu}(n,f)$ were measured relative to spontaneous fission neutron spectra (SFNS) of $^{252}\text{Cf}(sf)$. After various correction are applied to get absolute PFNS values, a number of systematic errors/uncertainties may appear, while the uncorrected cross ratios of various $^{233}\text{U}(n_{th},f)$, $^{235}\text{U}(n_{th},f)$ and $^{239}\text{Pu}(n_{th},f)$ PFNS pairs might be quite sterile in that respect.

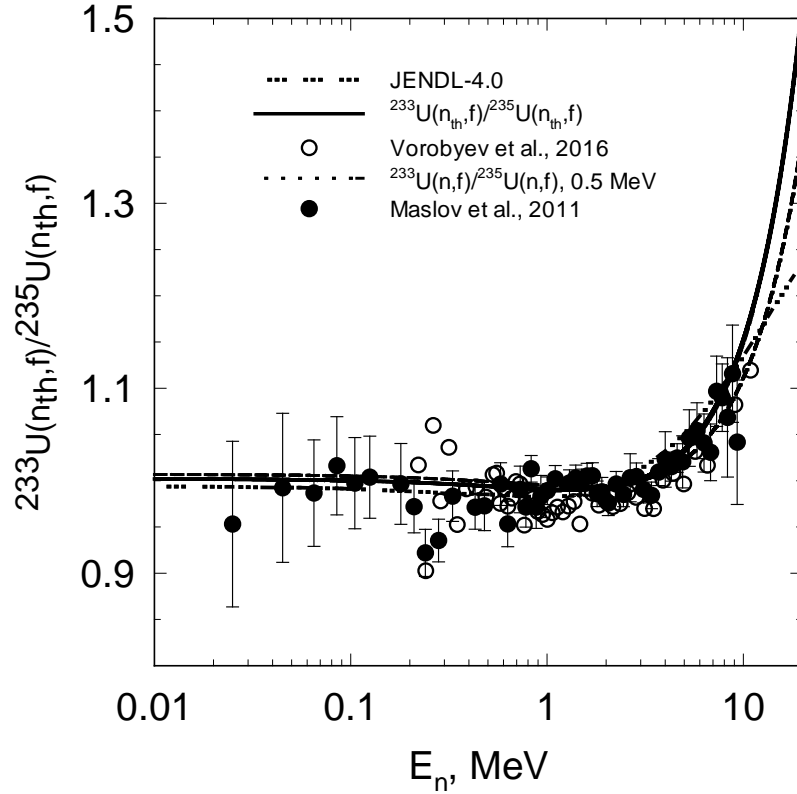


Fig. 2. Ratio of PFNS of $^{233}\text{U}(n_{th},f)$ and $^{235}\text{U}(n_{th},f)$ for thermal neutron-induced fission.

The ratios of PFNS for $^{239}\text{Pu}(n_{th},f)/^{233}\text{U}(n_{th},f)$ and $^{233}\text{U}(n_{th},f)/^{235}\text{U}(n_{th},f)$ [6, 7] and [4], contrary to absolute PFNS of $^{233}\text{U}(n_{th},f)$, $^{235}\text{U}(n_{th},f)$ and $^{239}\text{Pu}(n_{th},f)$, quite agree with each other (Fig. 2). At $E_n \sim E_{th}$ and $E_n \sim 0.5$ MeV the ratios of calculated PFNS of $^{239}\text{Pu}(n,f)$ and $^{235}\text{U}(n,f)$ in the range $0.01 < \varepsilon < 10$ MeV weakly depend on the E_n . Calculated PFNS ratios of [2, 3, 8, 14], as well as present calculation, at $E_n \sim E_{th}$ and $E_n \sim 0.5$ MeV almost coincide with PFNS ratios $^{239}\text{Pu}(n_{th},f)/^{233}\text{U}(n_{th},f)$ and $^{233}\text{U}(n_{th},f)/^{235}\text{U}(n_{th},f)$ of [4, 6, 7]. It might be concluded that the hardest prompt fission neutrons are emitted in $^{239}\text{Pu}(n_{th},f)$ reaction, while the softest PFNS is that of $^{235}\text{U}(n_{th},f)$, PFNS of $^{233}\text{U}(n_{th},f)$ takes intermediate position. Renormalization of model parameters at $E_n \sim E_{th}$ after fitting data on total kinetic energy of fission fragments [15] amounts to rather small changes of PFNS: for $^{239}\text{Pu}(n, f)$ a decrease by $\sim 2-3\%$ at $\varepsilon < 1$ MeV, for $^{235}\text{U}(n, f)$ and $^{233}\text{U}(n, f)$ PFNS - shifts by $\sim 1-2\%$ [2, 3].

$^{233}\text{U}(n, xnf)$ PROMPT FISSION NEUTRONS

Pre-fission neutrons emerging when $E_n \gtrsim E_{mf}$, influence the PFNS $S(\varepsilon, E_n)$ shape, total kinetic energy of fission fragments E_F^{pre} and fission products E_F^{post} , prompt fission neutron number $\nu_p(E_n)$, mass distributions and other fission observables. PFNS $S(\varepsilon, E_n)$ is a superposition of exclusive spectra of pre-fission neutrons, $(n, nf)^1$, $(n, nf)^1$, $(n, 2nf)^{1,2}$, $(n, 3nf)^{1,2,3} - d\sigma_{nxf}^k(\varepsilon, E_n)/d\varepsilon$ ($x=0, 1, 2, 3$; $k=1, \dots, x$), index x denotes the fission chance of $^{234-x}\text{U}$ and spectra of prompt fission neutrons, emitted by fission fragments, $S_{A+1-x}(\varepsilon, E_n)$:

$$\begin{aligned}
 S(\varepsilon, E_n) = & \tilde{S}_{A+1}(\varepsilon, E_n) + \tilde{S}_A(\varepsilon, E_n) + \tilde{S}_{A-1}(\varepsilon, E_n) + \tilde{S}_{A-2}(\varepsilon, E_n) = \\
 & \nu_p^{-1}(E_n) \cdot \left\{ \nu_{p1}(E_n) \cdot \beta_1(E_n) S_{A+1}(\varepsilon, E_n) + \nu_{p2}(E_n - \langle E_{nxf} \rangle) \beta_2(E_n) S_A(\varepsilon, E_n) + \right. \\
 & + \beta_2(E_n) \frac{d\sigma_{nxf}^1(\varepsilon, E_n)}{d\varepsilon} + \nu_{p3}(E_n - B_n^A - \langle E_{n2nf}^1 \rangle - \langle E_{n2nf}^2 \rangle) \beta_3(E_n) S_{A-1}(\varepsilon, E_n) + \beta_3(E_n) \cdot \\
 & \left. \left[\frac{d\sigma_{n2nf}^1(\varepsilon, E_n)}{d\varepsilon} + \frac{d\sigma_{n2nf}^2(\varepsilon, E_n)}{d\varepsilon} \right] + \nu_{p4}(E_n - B_n^A - B_n^{A-1} - \langle E_{n3nf}^1 \rangle - \langle E_{n3nf}^2 \rangle - \langle E_{n3nf}^3 \rangle) \cdot \right. \\
 & \left. \beta_4(E_n) S_{A-2}(\varepsilon, E_n) + \beta_4(E_n) \left[\frac{d\sigma_{n3nf}^1(\varepsilon, E_n)}{d\varepsilon} + \frac{d\sigma_{n3nf}^2(\varepsilon, E_n)}{d\varepsilon} + \frac{d\sigma_{n2nf}^3(\varepsilon, E_n)}{d\varepsilon} \right] \right\}. \tag{1}
 \end{aligned}$$

In equation (1) $\tilde{S}_{A+1-x}(\varepsilon, E_n)$ is lumped contribution of x -chance fission to the observed PFNS $S(\varepsilon, E_n)$, $\langle E_{nxf}^k \rangle$ – average energy of exclusive pre-fission neutron of $(n, xnf)^{1..x}$ reaction, spectra $S(\varepsilon, E_n)$, $S_{A+1-x}(\varepsilon, E_n)$ and $d\sigma_{nxf}^k(\varepsilon, E_n)/d\varepsilon$ are normalized to unity, $\beta_x(E_n) = \sigma_{n, xnf}(E_n)/\sigma_{n, F}(E_n)$ is the contribution of x -th fission chance $\sigma_{n, xnf}(E_n)$ to $\sigma_{n, F}$, $\nu_p(E_n)$ is the average number of prompt fission neutrons, $\nu_{px}(E_n)$ – average number of prompt fission neutrons, emitted by $^{234-x}\text{U}$ nuclides. PFNS, of neutrons, emitted from the fragments, $\tilde{S}_{A+1-x}(\varepsilon, E_n)$, as proposed in [16], were approximated by the sum of two Watt [17] distributions with different temperatures, the temperature of light fragment being higher.

The differential measured PFNS at $E_n \gtrsim E_{nxf}$ are also susceptible to systematic errors of various origin. In ratios of PFNS, especially of draft PFNS data, before corrections for the backgrounds, etc., these errors may be partially canceled [18, 19]. Figure 3 shows the $^{239}\text{Pu}(n, F)/^{235}\text{U}(n, F)$ and $^{233}\text{U}(n, F)/^{235}\text{U}(n, F)$ ratios of PFNS for $E_n \sim 7 \div 8$ MeV. The averaged $^{233}\text{U}(n, F)/^{235}\text{U}(n, F)$ ratio is very much different from that of $^{239}\text{Pu}(n, F)/^{235}\text{U}(n, F)$. The $^{239}\text{Pu}(n, F)/^{235}\text{U}(n, F)$ ratios of differential PFNS at $E_n \sim 7, 7.5$ and 8 MeV mildly, but significantly, fluctuate around averaged value. The respective $^{233}\text{U}(n, F)/^{235}\text{U}(n, F)$ ratios of PFNS also deviate from those of $^{239}\text{Pu}(n, F)/^{235}\text{U}(n, F)$. That is due to differing shapes of exclusive pre-fission (n, nf) spectra and $\beta_x(E_n)$ values. In the energy range of $E_n \sim 6 \div 7$ [19] the fluctuations of PFNS at $E_n \sim 6, 6.5$ and 7 MeV are more pronounced for both $^{239}\text{Pu}(n, F)/^{235}\text{U}(n, F)$ and $^{233}\text{U}/^{235}\text{U}(n, F)$ ratios, since competition of (n, nf) , $(n, 2n)$ and $(n, n\gamma)$ depends on excitation energy. The observed PFNS of $^{233}\text{U}(n, F)$ and $^{235}\text{U}(n, F)$ are similar, as the increase of contribution of $^{233}\text{U}(n, nf)$ is accompanied by decrease of $^{233}\text{U}(n, f)$ reaction contribution $S_{A+1}(\varepsilon, E_n)$.

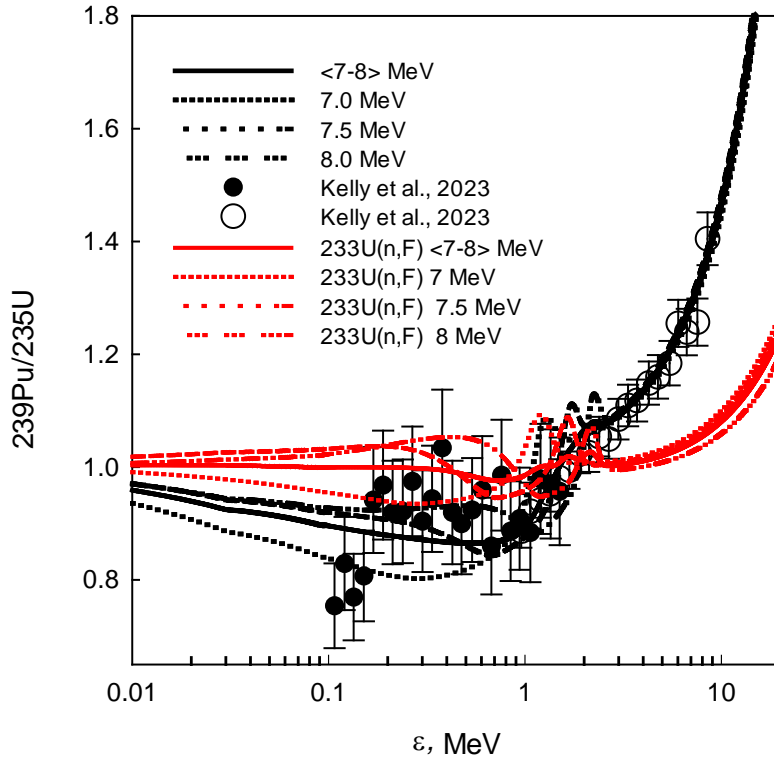


Fig.3. Ratios of PFNS $^{233}\text{U}(n,F)/^{235}\text{U}(n,F)$ and $^{239}\text{Pu}(n,F)/^{235}\text{U}(n,F)$ at $E_n \sim 6 \div 7$ MeV.

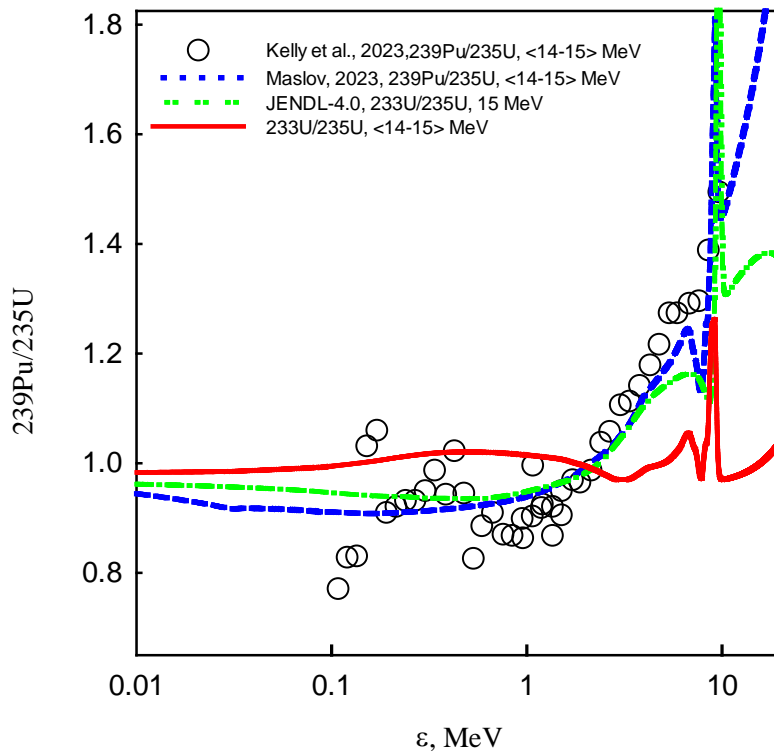


Fig.4. Ratios of PFNS $^{233}\text{U}(n,F)/^{235}\text{U}(n,F)$ and $^{239}\text{Pu}(n,F)/^{235}\text{U}(n,F)$ at $E_n \sim 14 \div 15$ MeV.

At $E_n \gtrsim E_{n2nf}$ integral emission spectrum of $(n,nX)^1$ reaction, $d^2\sigma_{nX}^1(\varepsilon, E_n)/d\varepsilon$, could be represented as a sum of compound and weakly dependent on neutron emission angle pre-equilibrium components, and phenomenological function, modelling energy and angle dependence of neutron spectra, relevant for the ^{233}U excitations of 1~6 MeV. Angle-averaged $\langle\omega(\theta)\rangle_\theta$ function, $\omega(\theta)$ [20], is approximated as $\langle\omega(\theta)\rangle_\theta \approx \omega(90^\circ)$, as described in [21]. Figure 4 compares calculated [20] and measured ratios of PFNS $^{239}\text{Pu}(n,F)/^{235}\text{U}(n,F)$ [20] and $^{233}\text{U}(n,F)/^{235}\text{U}(n,F)$ ratios at $E_n \sim 13 \div 14$ MeV. The latter calculated present ratio is much discrepant with that of JENDL-4.0 [13], which just follows the shape of $^{239}\text{Pu}(n,F)/^{235}\text{U}(n,F)$ of [13].

TKE values of E_F^{pre} are superposition of TKE for $^{234-x}\text{U}$ nuclides contributing to the observed fission cross section:

$$E_F^{pre}(E_n) = \sum_{x=0} E_{fx}^{pre}(E_{nx}) \beta_x(E_n) . \quad (2)$$

The excitation energy E_{nx} of $A, \dots, A+1-x$ nuclides, formed after emission of $(n, xn_f)^{1, \dots, x}$ pre-fission neutrons, depends on their average energies $\langle E_{nxf}^k \rangle$:

$$E_{nx} = E_r - E_{fx}^{pre} + E_n + B_n - \sum_{x=0, 1 \leq k \leq x} \left(\langle E_{nxf}^k \rangle + B_{nx} \right). \quad (3)$$

Kinetic energy E_F^{post} of fission products, which emerge after emission of pre-fission neutrons, but before β^- -decay, is defined as

$$E_F^{post} \approx E_F^{pre} \left(1 - \nu_{post} / (A+1 - \nu_{pre}) \right). \quad (4)$$

Weak variations of TKE values [15, 22], of both E_F^{pre} and E_F^{post} , in the vicinity of $^{233}\text{U}(n, xn_f)$ reaction thresholds are due to the decrease of excitation energy of $(A+1-x)$ fissioning nuclides after emission of x pre-fission neutron [23]. Contribution of $\sigma_{n, nf}$ to the $\sigma_{n, F}$ of $^{233}\text{U}(n, F)$, is larger than that of $^{235}\text{U}(n, nf)$ to the $\sigma_{n, F}$ of $^{235}\text{U}(n, F)$ [20, 24], nonetheless the local bumps in TKE around $^{233}\text{U}(n, 2nf)$ and $^{233}\text{U}(n, nf)$ reaction thresholds are weaker. That might be due to rather flat dependence on excitation energy of TKE for $^{232, 233, 234}\text{U}$, opposite to the case of TKE for $^{235, 236, 237, 238, 239}\text{U}$ fissioning nuclides. To reproduce the observed dependence of E_F^{pre} on E_n in $^{233}\text{U}(n, F)$ reaction one may assume linear dependence of first-chance fission TKE – $E_{f0}^{pre}(E_n)$ (Fig. 5).

Average energy of prompt fission neutron spectra is its rather rough signature. Figure 6 evidence that the shapes of $\langle E \rangle(E_n)$ in cases of $^{233}\text{U}(n, F)$ and $^{235}\text{U}(n, F)$ [20] are similar. Values of $\langle E \rangle$ are presented here in the interval $\varepsilon \sim 0.01 - 10$ MeV. Our estimate of $\langle E \rangle(E_n)$ for $^{235}\text{U}(n, F)$ [20] reproduces the estimate of $\langle E \rangle$ based on measured PFNS data [9, 26], especially around thresholds of $^{235}\text{U}(n, nf)$ and $^{235}\text{U}(n, 2nf)$ reactions.

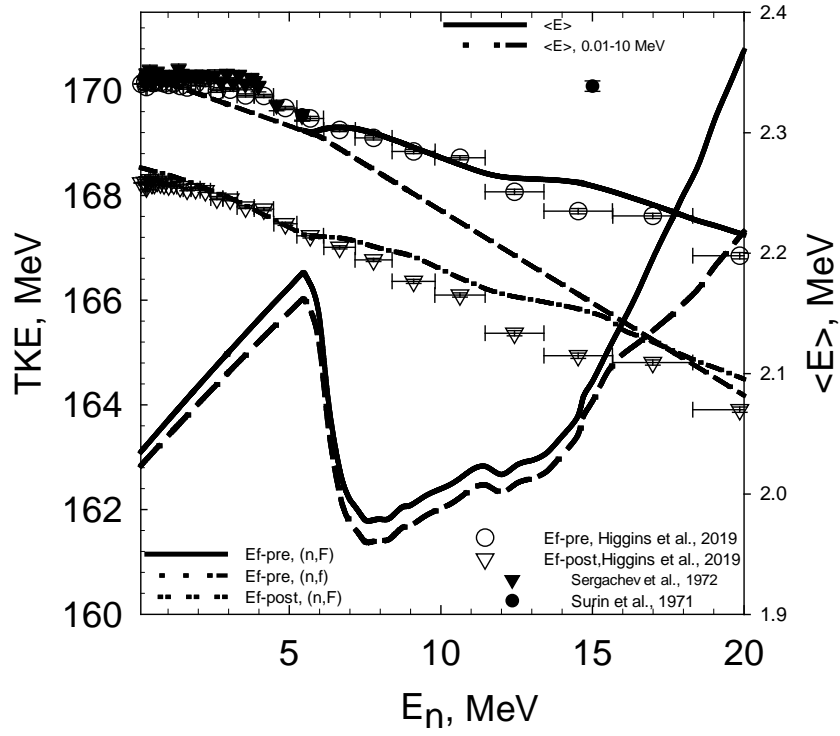


Fig. 5. Total kinetic energy TKE of $^{233}\text{U}(n,F)$.

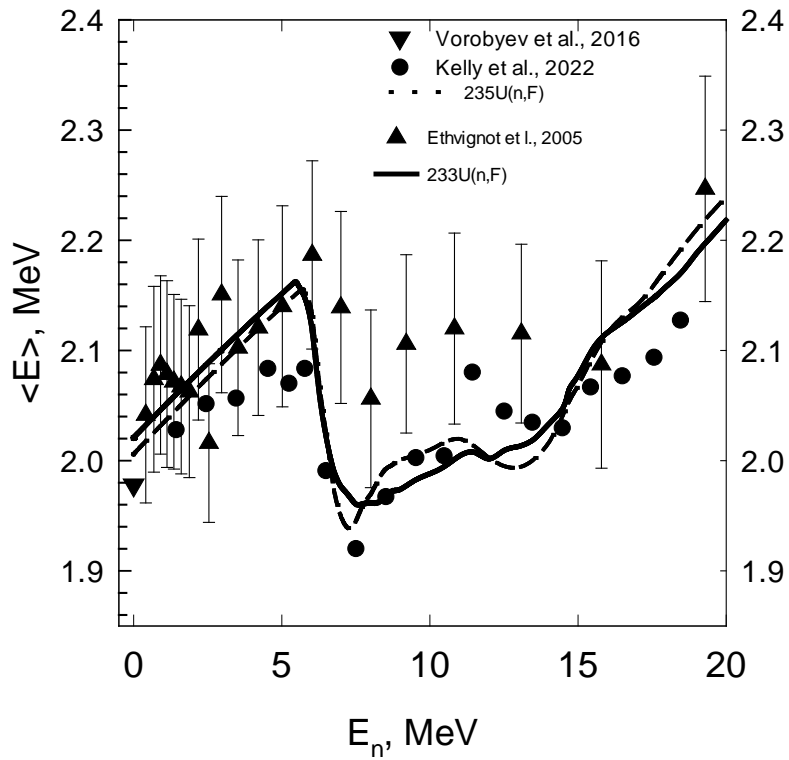


Fig.6. Average energy $\langle E \rangle$ of $^{233}\text{U}(n,F)$ and $^{235}\text{U}(n,F)$ PFNS.

CONCLUSION

A number of observed peculiarities in PFNS, TKE, $v_p(E_n)$ correlate with the emission of pre-fission (n, xnf) neutrons, as predicted for the $^{233}\text{U}(n, F)$ and $^{233}\text{U}(n, xnf)$ and earlier for $^{235}\text{U}(n, F)$ and $^{235}\text{U}(n, xnf)$ [20, 24]. Cross ratios of PFNS of $^{233}\text{U}(n, F)$, $^{235}\text{U}(n, F)$ and $^{239}\text{Pu}(n, F)$ reactions are compatible with measured data [11–13, 18, 19]. The correlation of PFNS shape and emissive ((n, xnf)) fission contribution to the observed fission cross section for $^{233}\text{U}(n, F)$ and $^{235}\text{U}(n, F)$ reactions is established. The net effect of these peculiarities is the occurrence of dips in $\langle E \rangle$ in the vicinity of (n, nf) and ($n, 2nf$) reaction thresholds and bumps in both E_F^{pre} and E_F^{post} . Amplitude of dips in $\langle E \rangle$ of $^{233}\text{U}(n, F)$ PFNS is quite similar to that observed in PFNS of $^{235}\text{U}(n, F)$ reaction, notwithstanding the appreciable differences of $^{233}\text{U}(n, xnf)$ and $^{235}\text{U}(n, xnf)$ reaction contributions to the observed fission cross sections $^{233}\text{U}(n, F)$ and $^{235}\text{U}(n, F)$, respectively. That is explained by relatively large contributions of $v_{px}(E_{nx})$ as compared with $v_{pre}(E_n)$ for the reaction $^{233}\text{U}(n, F)$. PFNS of $^{233}\text{U}(n, F)$ are more hard than those of $^{235}\text{U}(n, F)$ PFNS, but softer than those of $^{239}\text{Pu}(n, F)$. Difference of average energies of PFNS $\langle E \rangle$ of $^{233}\text{U}(n, F)$ and $^{235}\text{U}(n, F)$ amounts to 1~3 %. At incident energies higher than ($n, 2nf$) reaction threshold the observed PFNS may seem similar, though the partial contributions of $^{233}\text{U}(n, xnf)$ and $^{235}\text{U}(n, xnf)$ to the observed PFNS are quite different. It might be argued that correct estimate of the exclusive pre-fission (n, xnf) neutron spectra and modelling of spectra of neutrons emitted from excited fission fragments gives a robust prediction of PFNS for $^{233}\text{U}(n, F)$ for incident neutron energies $E_n \sim E_{th} - 20$ MeV with a precision and reliability comparable to those attained for $^{235}\text{U}(n, F)$ PFNS.

REFERENCES

1. Zamyatnin Yu.S., Saphina I.N., Gutnikova E.K., Ivanova N.I. Atom. Energ. 4, 337 (1958).
2. Maslov V. M., Baba M., Hasegawa A., Kagalenko A. B., Kornilov N.V., Teterova N.A. INDC (BLR) -18, IAEA, Vienna (2003), <https://www-nds.iaea.org/publications/indc/indc-blr-0018/>
3. Maslov V. M., Baba M., Hasegawa A., Kagalenko A. B., Kornilov N.V., Teterova N.A., Actinide neutron data, <https://www-nds.iaea.org/minskact>
4. Starostov B.I., Nefedov V.N., Boytsov A.A. Vopr. At. Nauki Techn., Ser. Nucl. Const. 4, 16 (1985).
5. Miura T, Baba M., Than Win, Ibaraki M., Hirasawa Y., Hiroishi T. and Aoki T. Journal of Nuclear Science and Technology. 39, 409 (2002).
6. Vorobyev A.S., Shcherbakov O.A. Vopr. At. Nauki Techn., Ser. Nucl. Const., 2, 52 (2016).
7. Vorobyev A.S., Shcherbakov O.A. Vopr. At. Nauki Techn., Ser. Nucl. Const., 1–2, 37 (2011).
8. Maslov V.M., Pronyaev V.G., Teterova N.A. et al In: Proc. Intern. Conf. Nuclear Cross Sections and Technology, Jeju, Korea, 2010, Journal of Korean Phys. Soc. 59, 1337 (2011).
9. Kelly K. J., Gomez J.A., Devlin M. et al. Phys. Rev. C, 105, 044615 (2022).

10. Kelly K. J., Devlin M., O'Donnell J.M. et al. Phys. Rev. C, 102, 034615 (2020).
11. Marini P., Taieb J., Laurent B. et al. Phys. Rev. C 101, 044614 (2020).
12. Chadwick M., Herman M., Obložinsky P. et al. Nuclear Data Sheets. 112, 2887 (2011).
13. Shibata K., Iwamoto O., Nakagawa T. et al. J. Nucl. Sci. Technol. 48, 1(2011).
14. Maslov V.M., In: LXXII International conference “Nucleus-2023”, Fundamental Problems and applications, Moscow, July, 11–16, 2022, Book of Abstracts, p.111, [https://events.sinp.msu.ru/event/8/attachments/181/875 nucleus-2022-book-of-abstracts-www.pdf](https://events.sinp.msu.ru/event/8/attachments/181/875/nucleus-2022-book-of-abstracts-www.pdf).
15. Higgins D., Greife U., Tovesson F., Manning B., Mayorov D., Mosby S., Schmitt K. Phys. Rev. C. 101, 014601 (2020).
16. Kornilov N.V., Kagalenko A.B., Hambsch F.-J. Yadernaya Fyzyka, 62, 209 (1999).
17. Watt B.E. Phys. Rev., 87, 1037 (1952).
18. Kelly K. J., Devlin M. J., O'Donnell M. et al. Phys. Rev. C 108, 024603 (2023).
19. Devlin M., Bennett E. A., Buckner M. Q., et al. In: Proceedings of the *International Conference Nuclear Data for Science and Technology, 24–29 July 2022, Sacramento, USA*; Eur. Phys. Journ. Web of Conf., 284, 04007 (2023).
20. Maslov V.M., Physics of Atomic Nuclei, 86, 627 (2023).
21. Maslov V.M., Physics of Particles and Nuclei Letters 20 (4), 565 (2023).
22. Sergachev A.I., Dyachenko P.P., Kovalev A.M., Kuzminov B.D., Yad. Fiz, 16, 475 (1972).
23. Maslov V.M., In: Proceedings of 29th International Seminar on Interaction of Neutrons with Nuclei: May 29 - June 2, 2023, JINR, Dubna, Russia, 2023, JINR, E3-2023-58, Dubna, 2023, p. 290–305.
24. Maslov V.M., Kornilov N.V., Kagalenko A.B., Teterova N.A Nucl. Phys. A, 760, 274 (2005).
25. Ethvignot T., Devlin M., Duarte H. et al. Phys. Rev. Lett. 94, 052701 (2005).